TÜBİTAK

Turk J Elec Eng & Comp Sci, Vol.19, No.3, 2011, © TÜBİTAK
doi:10.3906/elk-0908-176

ECG denoising on bivariate shrinkage function exploiting interscale dependency of wavelet coefficients

Sema KAYHAN, Ergun ERÇELEBİ*
Department of Electrical and Electronics Engineering, University of Gaziantep, 27310 Gaziantep-TURKEY
e-mails: {skoc,ercelebi}@gantep.edu.tr

Received: 05.09.2009

Abstract

This paper presents a new method for electrocardiogram (ECG) denoising based on bivariate shrinkage functions exploiting the interscale dependency of wavelet coefficients. Most nonlinear thresholding methods based on wavelet transform denoising assume that the wavelet coefficients are independent. However, wavelet coefficients of ECG signals have significant dependencies. In this paper, we proposed a new method by considering the dependencies between the coefficients and their parents in detail on a bivariate shrinkage function for denoising of an ECG signal corrupted by different types of noises, such as muscle artifact noise, electrode motion, and white noise. In real-time applications, reduction of computational time is very crucial, so we constructed the wavelet transform by lifting scheme. The lifting scheme is a new technique to construct wavelet transform; namely, second generation wavelet transform is an alternative and faster algorithm for a classical wavelet transform. The overall denoising performance of our proposed method was considered in relation to several measuring parameters, including types of wavelet filters (Daubechies 4 (DB4), Daubechies 6 (DB6), and Daubechies 8 (DB8)) and decomposition depth. Global performance was evaluated by means of the signal-to-noise ratio (SNR) and visual inspection. We used a set of MIT-BIH arrhythmia database ECG records. To evaluate our method, a comparative study was carried out that referred to effective data-driven techniques in the literature, namely VisuShrink, SureShrink, BayesShrink, and level-dependent threshold estimation. The experimental results indicated that the proposed methods in the paper were better than the compared methods in terms of retaining the geometrical characteristics of the ECG signal, SNR. Due to its simplicity and its fast implementation, the method can easily be used in clinical medicine.

Key Words: *Lifting scheme; bivariate shrinkage function; ECG denoising*

1. Introduction

The electrocardiogram (ECG) signal is a recording of the heart's electrical activity and provides valuable clinical information as to the heart's performance. The ECG was originally observed by Waller in 1899 [1].

*Corresponding author: Department of Electrical and Electronics Engineering, University of Gaziantep, 27310 Gaziantep-TURKEY

In 1903, Einthoven introduced electrophysiological concepts still in use today, including the labeling of the waves characterizing the ECG. He assigned the letters P through U to the waves, avoiding conflicts with other physiologic waves studied at that time. The ECG provides essential information to the cardiologist and is used for both monitoring and diagnostic purposes. It occupies a bandwidth of 0.05-150 Hz. A typical ECG monitoring device generates large amounts of digital data. Each data sample may have 8-, 12-, or 16-bit resolution. This will lead to an accumulation of ECG data ranging from 60 Kb/min to 480 Kb/min [2].

ECG records are often contaminated by various artifacts. The sources of artifacts can be cardiac-related, such as reduction or disappearance of the isoelectric interval, prolonged repolarization, or atrial flutter. Extracardiac sources include physical movement, changes of electrode contact position, respiration, muscle contraction, and power line interference. The spectrum of artifacts spans low to high frequency components. Baseline wander due to respiration contains low frequency components; power line interference and muscle contraction contain high frequencies. Motion artifacts usually generate high amplitude spikes. Moreover, for emergency medicine, early diagnosis by a specialist in an ambulance is vitally important. Telemedicine is a useful technique for remote medical care. Different communication tools such as the telephone line, mobile communication, and satellite communication are available. The ECG is one of the most important vital signs to be transmitted in emergency care. While an ECG is being transmitted from a remote area to a health care center, if the communication link is not good, noise appears in the received ECG. These different sources of noise considerably prevent the accurate analysis of the ECG signal and the eventual diagnosis of cardiac anomalies.

Removal of noises is the first and crucial step in the detection of ECG waves for cardiac disease diagnosis. A good performance of an ECG-analyzing system depends heavily upon the accurate and reliable detection of the QRS complex, as well as the T- and P-waves.

Much work had been carried out on denoising algorithms. Some of them, however, either use linear or nonlinear filters, such as the median filter [3]. The median filter fails to remove Gaussian noise without distorting the characteristics of the ECG signal [4]. On the other hand, linear filtering removes both the noise and the high frequency components of the ECG signal in the case of the noise overlapping with the high frequency components of the ECG, and the ECG then becomes blurred. For example, the most straightforward solution to the problem of denoising an ECG signal is to apply a constant coefficient digital filter. The problem with this approach is that one cannot choose a satisfactory cutoff frequency for the filter. If the cutoff is chosen to be too large, then not enough noise will be filtered off, leading to difficulties in extracting P- and T-wave parameters. As the cutoff frequency is reduced, so too will be the noise content, but high frequency features of the ECG, such as the R-wave, will start to be filtered, leading to distortion of the ECG because the frequency bands of the noises often overlap with those of the QRS complex. The other most widely used technique for denoising an ECG signal is averaging [5, 6]. A major disadvantage in signal averaging is that it tends to remove short term changes in the ECG waveform. Furthermore, a single ECG complex of poor quality may have an excessive influence or indeed distort the resulting ECG average. To avoid this, only ECG complexes that satisfy a suitable quality criterion are included in the averaging process. However, this may distort the information. Furthermore, the existence of significantly large low frequency noise components that are correlated, such as baseline shifts, serve to reduce the effectiveness of averaging.

An alternating solution to the abovementioned ECG denoising methods is the wavelet-based ECG denoising method. At present, there are mainly 2 kinds of wavelet denoising methods used in the denoising of ECG signals: one is the wavelet transform modulus maxima method [7, 8]. This method can eliminate noises and retain the information of the original signal in maximum at the same time, but the amount of calculation is great and the process of calculation may be unstable [9, 10]. The other is the wavelet thresholding denoising method

proposed by Donoho and Johnston [11-14]. The wavelet thresholding denoising method deals with wavelet coefficients using a suitable threshold chosen in advance. The wavelet coefficients at different scales could be obtained by taking the discrete wavelet transform (DWT) of the noisy signal. A thresholding method compares the wavelet coefficient with the threshold value and is set to 0 if its magnitude is less than the threshold value; the others with larger magnitudes than the present threshold are mainly assumed to be caused by the original signal and are kept. Then the denoised signal can be reconstructed from the resulting wavelet coefficients. Different studies recently done for ECG denoising based on wavelet thresholding indicate that they are dealing with different parameters of the thresholding process, such as selection of the wavelet filters and computation of the threshold value. The computation of the threshold value is truly essential for good performance of the wavelet-based ECG denoising methods. In [11], Donoho proposed a threshold estimator method, which is known as a universal threshold. This threshold estimator depends on the length of the signal samples. If the number of signal samples is too small, the result will still be noisy. On the other hand, if too large, important ECG signals will be removed. To overcome the disadvantage mentioned above, in [14] the level-dependent threshold estimator proposed by Johnstone and Silverman was used. Other approaches for threshold value estimators can be found in [15, 16]. VisuShrink [11, 15] utilizes the universal threshold estimator, which is $\sqrt{2\log(N)}$ for a vector d_i of the detail coefficients of length N. SureShrink is based on Stein's unbiased risk estimator [17]. SureShrink has serious drawbacks in situations of extreme sparsity of the wavelet coefficients [18]. In [11], BayesShrink was used for the threshold estimator, which is a data-driven subband adaptive technique.

In this paper, we propose a new method for denoising ECG signals in the lifting-based wavelet domain. The method uses bivariate probability distribution functions (pdfs) and corresponding shrinkage functions based on Bayesian estimation theory, especially the maximum a posteriori (MAP) estimator. The wavelet shrinkage considered here was conceptually inspired by the work of Şendur and Selesnick [19], who developed a wavelet shrinkage method for the denoising of 2D images. The wavelet shrinkage methods that are available in the literature [20-25] ignore the dependencies between wavelet coefficients in scale i^{th} and $(\mathrm{i}+1)^{th}$. However, the wavelet coefficients are statistically dependent [26] due to 2 properties of the wavelet transform: 1) if a wavelet coefficient is large/small, the adjacent coefficients are likely to be large/small, and 2) large/small coefficients tend to propagate across scales [19].

The proposed method considers not only that wavelet coefficients are statistically dependent, but also that they have statistically Gaussian distributions. In addition, the method utilizes a lifting scheme to construct the wavelet transform, because the construction of the wavelet transform by lifting scheme requires less computational time. In real-time application, reduction of computational time is very crucial. The proposed ECG denoising method showed improved output SNR values compared to a set of tested level-dependent threshold estimations proposed in [14], VisuShrink, SureShrink, and BayesShrink for the denoising process, as will be explained in more detail throughout the paper.

The paper is organized as follows: Section 2.1 introduces the ECG signal. Section 2.2 presents lifting-based wavelet transform. Section 2.3 describes the ECG denoising method based on bivariate shrinkage function. The implementation of the denoising of an ECG is presented in Section 2.4, together with a discussion of the advantages of the present implementation in comparison with VisuShrink, SureShrink, BayesShrink, and level-dependent threshold estimation. Finally, Section 3 considers the utility of the method and its limitations.

2. Materials and methods

2.1. ECG signal

Figure 1 shows a typical ECG signal. The first ECG wave within the cardiac cycle is the P-wave, reflecting atrial depolarization. Its duration is about 90 ms. It is a positive wave whose amplitude is normally lower than or equal to 0.2 mV. Depolarization of the ventricles is represented by the QRS complex. Its normal duration lies between 85 and 95 ms. Following the QRS complex, another segment, the ST interval, is observed. The ST interval represents the duration of depolarization after all ventricular cells have been activated. After completion of the ST segment, the ventricular cells return to their electrical and mechanical resting state, completing the repolarization phase observed as a low frequency component known as the T-wave.

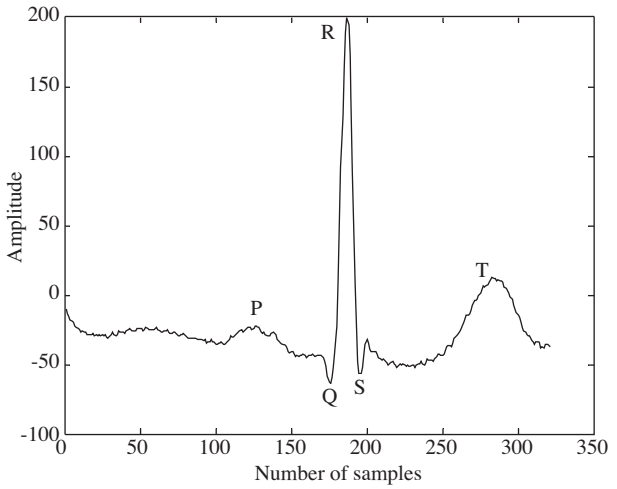

Figure 1. Typical ECG signal with P-wave, QRS complex, and T-wave (sampling frequency is 360 Hz).

In order to evaluate the performance of this new denoising method, we used the MIT-BIH arrhythmia database [27, 28]. We selected a subset of 3 signals (MIT-BIH database records 103, 109, and 117) of 10 min in length. The sampling frequency of these signals is 360 Hz and they have a resolution of 11 bits per sample.

2.2. Lifting-based wavelet transform

Wavelet applications have increasingly gained in importance over the last decade. However, the computational complexity for calculating dyadic wavelet transforms is very high**.** In order to satisfy the demand for real-time signal processing applications, improving the hardware implementations of the discrete wavelet transform (DWT) has become very important. The dyadic wavelet transform can be considered as a subband transform, implemented with iterated filter banks with down-sampling operations [29]. Figure 2 shows the general block scheme of a 1-dimensional wavelet transform. The forward transform uses 2 analysis filters, $\tilde{h}$ (low-pass) and $\tilde{g}$ (high-pass), followed by subsampling. The combination of these filters, h and g, is used for reconstruction of the signal. These filters are chosen in such a way that the perfect reconstruction criterion is satisfied. The outputs of the synthesis filters are added together to reconstruct the original signal.

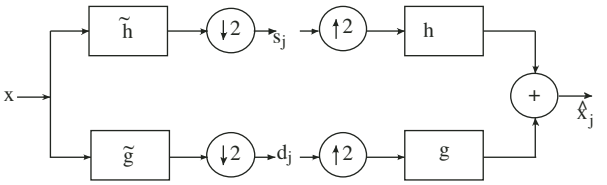

Figure 2. Classical wavelet transform.

One problem associated with wavelet-based ECG denoising is the high computational complexity.

It is very crucial to speed up the computation of the wavelet transform for real-time ECG denoising, especially for long-recorded ECG signals. The conventional convolution-based implementation of the discrete wavelet transform (DWT) has high computational and memory requirements [30]. Recently, the lifting-based implementation of DWT [31-33] has been proposed to overcome these drawbacks. It is fast and consumes relatively little memory. As shown in Figure 3, the lifting scheme consists of (1) splitting an original sequence into an even and an odd sequence, (2) subtracting the prediction estimated by the even sequence from the odd sequence, and (3) updating the even sequence in order to avoid alias effects [14, 34]. These procedures consequently render the even sequence the coefficients of scaling function, and the odd sequence the wavelet coefficients.

Consider a signal $s = (s_k)_{k \in Z}$ with $s_k \in R$. The signal is split into points with an odd and even index, as in Figure 3 [31]. The even-indexed samples are $s_e = (s_{2k})_{k \in Z}$ and the odd-indexed samples are $s_{o=}(s_{2k+1})_{k \in Z}$. The even samples are an approximation of the original signal and are used to recover the original signal. The even samples s_{2k} can immediately be found as $s_{2k} = s_e$. We can predict the odd samples based on the s_o by assuming an odd sample s_o as the average of its 2 (even) neighbors, s_{2k} and s_{2k+1}. Therefore, the even samples are used as a predictor for the odd set.

$$\gamma = s_e - P(s_o) \tag{1}$$

If the detail d and the odd set are given, the even set can immediately be recovered as

$$s_e = P(s_o) + \gamma. \tag{2}$$

The wavelet coefficient γ_k is the difference between the exact sample and its predicted value.

$$\gamma = s_{2k+1} - (s_{2k} + s_{2k+1})/2 \tag{3}$$

The process of computing a prediction and recording it is called a lifting step. In this way, the original signal is transformed from (s_e, s_o) to (s_e, s_Y). Since s_e is obtained by simply subsampling the even samples, serious aliasing takes place. To overcome this, a second lifting step is introduced, in which the even samples are replaced with smoothed values with the use of an update operator U applied to the details [32].

$$S = s_e + U(\gamma) \tag{4}$$

$$s_e = S - U(\gamma) \tag{5}$$

The block diagram of the 2 lifting steps is given in Figure 3. It is easy to see that an update operator reduces aliasing. The wavelet constructed by the lifting scheme does not need to be translated or dilated.

$$\lambda_k = s_{2k} + (\gamma_{k-1} + \gamma_k)/4 \tag{6}$$

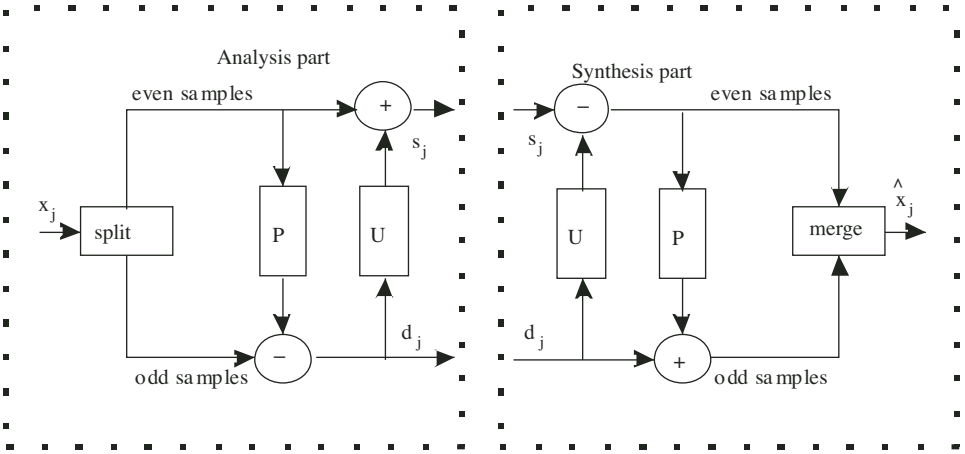

Figure 3. Lifting scheme: a) forward transform, b) inverse transform.

The unit used is the cost in the comparison of computational complexity of the lifting-based wavelet transform with that of classical wavelet transform, measured in the number of multiplications and additions of computing 1 sample pair, (s_l, d_l). Here s_l represents approximation coefficients and d_l indicates detail coefficients. Take $\left|\tilde{h}\right| = 2N, \quad |\tilde{g}| = 2M$. The cost of the classical wavelet transform is $4(N+M)+2$, while the cost of the lifting algorithm is $2(N+M+2)$. Table 1 lists the computational cost L of lifting-based wavelet transform with that S of classical wavelet transform and the relative speedup, $\left(\frac{S}{L}-1\right)$ [31].

Table 1. The computational cost of lifting-based wavelet transform with that of classical wavelet transform and the relative speedup.

Wavelet	The number of multiplications and additions for classical wavelet transform	The number of multiplications and additions for lifting-based avelet transform	Speedup (%)
Haar	10	8	25
DB4	34	20	70
DB6	50	28	78
DB8	66	36	83

It is clear from Table 1 that as the order of the filter increases, the computational cost decreases.

Lifting schemes can also be used to factor all of the polyphase matrices that represent a wavelet transform with finite filters into a finite product of upper and lower triangular matrices and a diagonal normalization matrix. To factor the wavelet filters into lifting steps, the low-pass $(\tilde{h}[z], h[z])$ and high-pass $(\tilde{g}[z], g[z])$ filters are first separated into even and odd parts.

$$\begin{aligned} \tilde{h}[z] &= \tilde{h}_e\left[z^2\right] + z^{-1}\tilde{h}_0\left[z^2\right] \\ \tilde{g}[z] &= \tilde{g}_e\left[z^2\right] + z^{-1}\tilde{g}_0\left[z^2\right] \end{aligned} \tag{7}$$

$$\begin{aligned} h[z] &= h_e\left[z^2\right] + z^{-1}h_0\left[z^2\right] \\ g[z] &= g_e\left[z^2\right] + z^{-1}g_0\left[z^2\right] \end{aligned} \tag{8}$$

The polyphase matrices are then defined as below.

$$\tilde{P}[z] = \begin{bmatrix} \tilde{h}_e[z] & \tilde{h}_0[z] \\ \tilde{g}_e[z] & \tilde{g}_0[z] \end{bmatrix} \tag{9}$$

$$P[z] = \begin{bmatrix} h_e[z] & g_e[z] \\ h_0[z] & g_0[z] \end{bmatrix} \tag{10}$$

Using the Euclidean algorithm, which recursively finds the greatest common divisors of the even and odd parts of the original filters, $\tilde{P}[z]$ can always be factored into lifting steps, as follows:

$$P[z] = \begin{bmatrix} K_1 & 0 \\ 0 & K_2 \end{bmatrix} \prod_{i=1}^{m} \begin{bmatrix} 1 & \tilde{s}_i[z] \\ 0 & 1 \end{bmatrix} \begin{bmatrix} 1 & 0 \\ \tilde{t}_i[z] & 1 \end{bmatrix}. \tag{11}$$

Equation (11) is the polyphase decomposition and $\tilde{P}[z]$ is the polyphase matrix. By factoring the existing wavelets into lifting steps, the computational complexity can be reduced by up to 50% compared to the traditional direct convolution-based implementation. Hence, lifting-based hardware implementations provide a more efficient way to compute wavelet transforms [35].

The 4-tap orthonormal filter (DB4) is chosen to illustrate polyphase factorization:

$$\tilde{h}(z) = h_0 + h_1 z^{-1} + h_2 z^{-2} + h_3 z^{-3} \tag{12}$$

$$\tilde{g}(z) = -h_3 z^2 + h_2 z - h_1 + h_0 z^{-1}, \tag{13}$$

where

$$h_0 = \frac{1+\sqrt{3}}{4\sqrt{2}}, \quad h_1 = \frac{3+\sqrt{3}}{4\sqrt{2}}, \quad h_2 = \frac{3-\sqrt{3}}{4\sqrt{2}}, \quad h_3 = \frac{1-\sqrt{3}}{4\sqrt{2}}. \tag{14}$$

The polyphase matrix is

$$\tilde{P}(z) = \begin{bmatrix} h_0 + h_2 z^{-1} & -h_3 z - h_1 \\ h_1 + h_3 z^{-1} & h_2 z + h_0 \end{bmatrix}. \tag{15}$$

Applying a Euclidean algorithm to Laurent polynomials, the factorization is obtained as follows:

$$\tilde{P}(z) = \begin{bmatrix} 1 & -\sqrt{3} \\ 0 & 1 \end{bmatrix} \begin{bmatrix} 1 & 0 \\ \frac{\sqrt{3}}{4} + \frac{\sqrt{3}-2}{4} z^{-1} & 1 \end{bmatrix} \begin{bmatrix} 1 & z \\ 0 & 1 \end{bmatrix} \begin{bmatrix} \frac{\sqrt{3}+1}{\sqrt{2}} & 0 \\ 0 & \frac{\sqrt{3}-1}{\sqrt{2}} \end{bmatrix}. \tag{16}$$

2.3. ECG denoising method based on bivariate shrinkage function

Most simple wavelet-based nonlinear thresholding models assume that the wavelet coefficients are independent and try to characterize them by Gaussian, Laplacian, generalized Gaussian, or other distributions [19, 36]. For example, the conventional ECG denoising method is a soft thresholding scheme, which is a nonlinear threshold method proposed on the assumption of wavelet coefficients' independence without considering the dependency between wavelet coefficients. However, algorithms exploiting dependencies between coefficients for modeling probability density function (pdf) of wavelet coefficients can achieve better results for ECG signal

denoising in the wavelet domain, compared with the ones based on the independence assumption. In [19], a bivariate pdf is used to model the interscale dependencies of wavelet coefficients, showing that algorithms that use a bivariate pdf instead of a univariate pdf have better results for wavelet-based image denoising. Marginal models cannot model the statistical dependencies between wavelet coefficients, so in this paper, a jointly non-Gaussian model, $p_w(w)$, is used to characterize the dependency between a coefficient and its parent, and derives the corresponding bivariate MAP estimators based on noisy wavelet coefficients in detail. The bivariate shrinkage function based on the dependency between wavelet coefficients is derived from the Bayesian maximum a posteriori (MAP) estimation theory and applied to ECG signals.

The noise corrupting the ECG signals is considered as white Gaussian noise. We observed (a noisy signal) and wished to estimate the desired signal as accurately as possible according to some criteria.

The problem can be formulated as follows.

Let w_2 represent the parent of w_1, which is the wavelet coefficient at the same position as w_1, but at the next coarser scale. Then

$$\begin{aligned} z_1 &= w_1 + n_1 \\ z_2 &= w_2 + n_2 \end{aligned}, \tag{17}$$

where z_1 and z_2 are the noisy wavelet coefficients, w_1 and w_2 are the noise-free wavelet coefficients, and n_1 and n_2 are the noise wavelet coefficients. We can write

$$\mathbf{z} = \mathbf{w} + \mathbf{n}, \tag{18}$$

where $\mathbf{w} = \{w_1, w_2\}$, $\mathbf{z} = \{z_1, z_2\}$, and $\mathbf{n} = \{n_1, n_2\}$. Given the corrupted observation $\mathbf{z}$, the standard MAP estimator [12] for $\mathbf{w}$ is

$$\hat{\mathbf{w}}(\mathbf{z}) = \arg\max_{\mathrm{w}} \left[P_{\mathbf{w}|\mathbf{z}}(\mathbf{w}|\mathbf{z})\right]. \tag{19}$$

By using Bayesian maximum a posteriori (MAP) estimation theory, this equation can be written as

$$\hat{\mathbf{w}}(\mathbf{z}) = \arg\max_{\mathbf{w}} \left[P_{\mathbf{z}|\mathbf{w}}(\mathbf{z}|\mathbf{w}) \cdot P_{\mathbf{w}}(\mathbf{w})\right] \quad = \arg\max_{\mathbf{w}} \left[P_{\mathbf{n}}(\mathbf{z}-\mathbf{w}) \cdot P_{\mathbf{w}}(\mathbf{w})\right]. \tag{20}$$

Here, $P_{\mathbf{n}}(\mathbf{n})$ is the probability density function (pdf) of the wavelet coefficients of the noise and $P_{\mathbf{w}}(\mathbf{w})$ is the pdf of the wavelet coefficients of a noise-free signal. To evaluate the original signal from the observation signal, the value of $P_{\mathbf{n}}(\mathbf{n})$ and $P_{\mathbf{w}}(\mathbf{w})$ should be obtained.

It is clear from equation (20) that the Bayes rule allows us to write this estimation in terms of the probability densities of noise and the prior density of the wavelet coefficients. In order to use this equation to estimate the original signal, we must know both pdfs. The pdf for the wavelet coefficients of the noise is often modeled as i.i.d. Gaussian with zero mean and variance σ_n.

$$p_{\mathbf{n}}(\mathbf{n}) = \frac{1}{2\pi\sigma_n^2} \cdot \exp\left(-\frac{n_1^2 + n_2^2}{2\sigma_n^2}\right) \tag{21}$$

The joint empirical coefficient-parent histogram can be used to observe $P_{\mathbf{w}}(\mathbf{w})$ (22). The pdf of the noise-free wavelet coefficients is given as in [19]; with this pdf, w_1 and w_2 are uncorrelated but not independent.

$$P_{\mathbf{w}}(\mathbf{w}) = \frac{3}{2\pi\sigma^2} \exp\left(-\frac{\sqrt{3}}{\sigma}\sqrt{w_1 + w_2}\right). \tag{22}$$

Equation (20) is equivalent to

$$\hat{\mathbf{w}}(z) = \arg\max_{\mathbf{w}} \left[\log(p_{\mathbf{n}}(\mathbf{z}-\mathbf{w}) + \log(p_{\mathbf{w}}(\mathbf{w})\right]. \tag{23}$$

Let us define $f(\mathbf{w}) = \log(p_{\mathbf{w}}(\mathbf{w}))$. Using equation (21), equation (23) becomes

$$\hat{\mathbf{w}}(\mathbf{z}) = \arg\max_{\mathbf{w}} \left[-\frac{(z_1 - w_1)^2}{2\sigma_n^2} - \frac{(z_2 - w_2)^2}{2\sigma_n^2} + f(\mathbf{w}) \right]. \tag{24}$$

It corresponds to the solution of the following equations for $\hat{w}_1$ and $\hat{w}_2$:

$$\frac{z_1 - \hat{w}_1}{\sigma_n^2} + f_1'(\mathbf{w}) = 0 \tag{25}$$

$$\frac{z_2 - \hat{w}_2}{\sigma_n^2} + f_2'(\mathbf{w}) = 0, \tag{26}$$

where f_1 and f_2 represent the derivative of $f(\mathbf{w})$ w.r.t. w_1 and w_2, respectively. From equation (22), $f(\mathbf{w})$ can written as

$$f(\mathbf{w}) = \log\left(\frac{3}{2\pi\sigma^2}\right) - \frac{\sqrt{3}}{\sigma}\sqrt{w_1 + w_2}. \tag{27}$$

From this,

$$\begin{array}{l} f_1'(\mathbf{w}) = -\frac{\sqrt{3}w_1}{\sigma\sqrt{w_1^2+w_2^2}} \\ \\ f_2'(\mathbf{w}) = -\frac{\sqrt{3}w_2}{\sigma\sqrt{w_1^2+w_2^2}} \end{array} . \tag{28}$$

Solving equations (25) and (26) using equation (28), the joint shrinkage function (or the MAP estimator) can be written as

$$\hat{w}_1 = \frac{\left(\sqrt{z_1^2 + z_2^2} - \frac{\sqrt{3}\sigma_n^2}{\sigma}\right)_+}{\sqrt{z_1^2 + z_2^2}} \cdot z_1. \tag{29}$$

Here, $(g)_+$ is defined as

$$(g)_+ = \begin{cases} 0, & g < 0 \\ g, & \text{others} \end{cases} . \tag{30}$$

This equation is equivalent to the classical soft shrinkage.

$$\hat{w}_1(z) = \begin{cases} 0, \ if \left(\sqrt{z_1^2 + z_2^2} - \frac{\sqrt{3}\sigma_n^2}{\sigma}\right) < 0 \\ \\ \left(\frac{\sqrt{z_1^2+z_2^2} - \frac{\sqrt{3}\sigma_n^2}{\sigma}}{\sqrt{z_1^2+z_2^2}} z_1\right), \ \text{otherwise} \end{cases} \tag{31}$$

Bivariate models are based on strong dependencies between a coefficient and its parent in detail. To estimate the noise variance from noisy wavelet coefficients, a robust median estimator is used from the finest scale wavelet coefficients:

$$\sigma_n^2 = \frac{median\left(|z_i|\right)}{0.6745}. \tag{32}$$

Algorithm for proposed method:

Step 1: Decompose noisy ECG signal into subbands by forward lifting-based wavelet transform.
Step 2: Compute the noise variance using the robust median estimator given in equation (32).
Step 3: Process each subband separately:

- Compute signal variance σ^2 and the threshold value.
- Compute denoised wavelet coefficient by using the bivariate shrinkage function given in equation (31).

Step 4: Reconstruct the signal by the inverse lifting wavelet transform.

2.3. Experimental study

In order to evaluate the performance of the proposed method, we conducted some experiments and compared them with the results of VisuShrink, SureShrink, BayesShrink, and level-dependent threshold estimation. In our experiments, we used actual ECG records (103, 109, and 117) from the MIT-BIH arrhythmia database and 3 different kinds of noise: simulated white noise, electrode motion artifact noise, and muscle artifact noise. Since the ECG data records were very long, we considered the segment (the number of samples in a segment is 1300) of ECG data records. The lifting-based wavelet transform included in the study belonged to the following families: Daubechies (DB4, DB6, DB8). White Gaussian noise of different standard deviations was artificially generated, but 2 records of physiological noise, electrode motion ('em') and muscular activity noise ('ma'), were taken from the MIT-BIH arrhythmia database. We utilized the output SNR value between the constructed denoised ECG signal and the noise-free signal as well as the visual inspection to evaluate the denoising algorithm. The performances of the ECG signal in the presence of the interference noise were evaluated for different signal-to-noise ratios (SNR).

The output SNR:

The output SNR was calculated as follows:

$$SNR_{out} = 10 \log \left(\frac{\sum_{i=1}^{N} x_r^2(i)}{\sum_{i=1}^{N} (x_r - x_d)^2} \right), \tag{33}$$

where x_r denotes the noise-free ECG signal and x_d represents the denoised ECG signal, whereas N is the length of the data segment (1300 in our approach).

Figures 4a and 4b denote clean ECG signals (MIT-BIH database record 103) and the corrupted ECG with white Gaussian noise at SNR 6.8 dB, while Figures 4c-4f show the results of the proposed method and the others, respectively.

Figure 5a illustrates the corrupted ECG with electrode motion artifact noise at SNR = 12.81 dB. Figures 5b-5f show the denoised ECG signal resulting from the proposed method and the others, respectively. The noise removed at different decomposition levels was investigated using the wavelets DB4, DB6, and DB8. The proposed method at different levels (second, third, and fourth) was applied to the noisy ECG signal. We noted that increasing the decomposition level had no effect on improving the SNR.

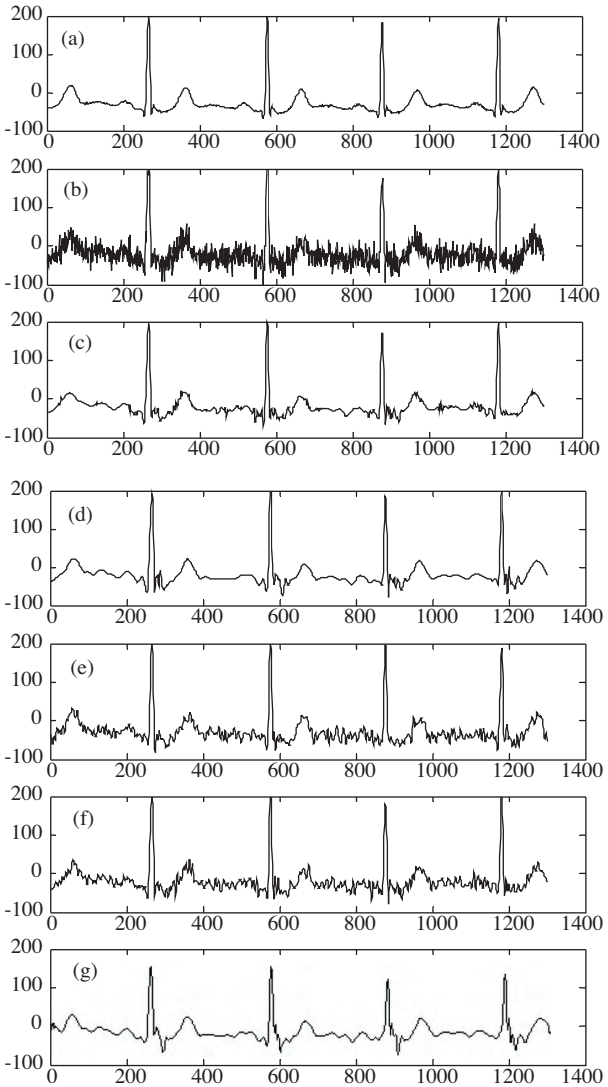

Figure 4. a) Original ECG signal (MIT-BIH database record 103), b) corrupted ECG signal by Gaussian noise at SNR = 6.8 dB, c) result of proposed method with Daubechies 8 at SNR = 12.0381 dB, d) result of VisuShrink at SNR = 10.50 dB, e) result of BayesShrink at SNR = 10.8212 dB, f) result of SureShrink at SNR = 10.5488 dB, g) result of level-dependent threshold estimator at SNR = 8.7608 dB.

Figure 6a shows the ECG signal (MIT-BIH database record 103) corrupted by motion artifact noise with SNR = 12.81 dB. Figures 6b-6g show the denoised ECG signals by the proposed method with DB8 filter, VisuShrink, SureShrink, BayesShrink, and level-dependent threshold estimation, respectively. From Figure 6c, it can be seen that bivariate shrinkage using LBWF is better in retaining the characteristics of the original ECG signal and the loss of the amplitudes of R-waves is not obvious, but it can hardly suppress the impulse noise. Moreover, it can be seen from Figures 6d-6g that the denoising method proposed in this paper is superior to the other denoising methods in comprehensive performance.

The results demonstrate the robustness of the proposed method among the different denoising methods for nonstationary noises.

Table 2 presents the SNR between the denoised ECG signal and the clean ECG signal, as obtained for each method. The ECG signal was corrupted by adding white Gaussian noise. The noise level was adjusted to specific values in such a way as to obtain the different SNRs. Lifting-based DB4, DB6, and DB8 wavelet filters, bivariate shrinkage, and decomposition level 4 were used by the proposed algorithm in Table 2.

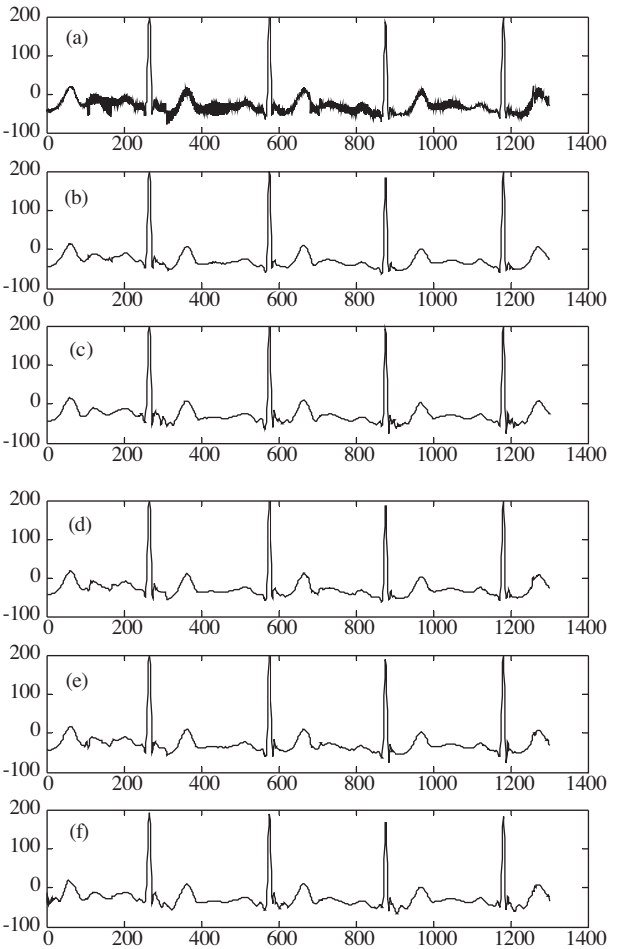

Figure 5. a) Corrupted ECG signal (MIT-BIH database record 103) by electrode motion artifact noise at SNR = 12.81 dB, b) result of proposed method with Daubechies 8 at SNR = 16.7872 dB, c) result of VisuShrink at SNR = 15.7494 dB, d) result of BayesShrink at SNR = 16.6036 dB, e) result of SureShrink at SNR = 16.1404 dB, f) result of level-dependent threshold estimator with Daubechies 8 at SNR = 15.0277 dB.

Table 3 lists the SNR of the proposed method and the other methods for the ECG signals (MIT-BIH database record 103) corrupted with electrode motion artifact noise. In Table 3, different kinds of lifting-based wavelet filters (DB4, DB6, DB8) were used with the proposed method.

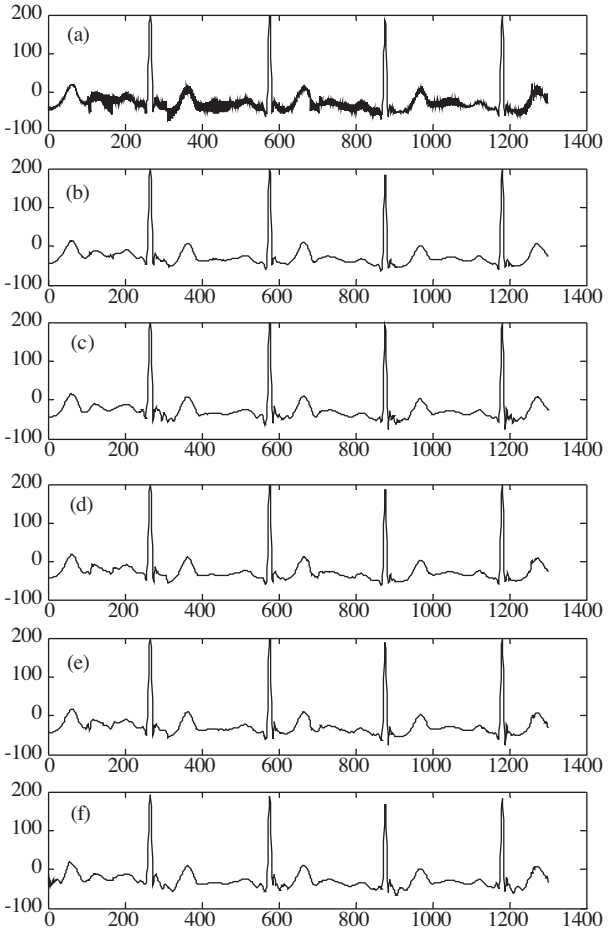

Figure 6. a) Corrupted ECG signal (MIT-BIH database record 103) by motion artifact noise at SNR = 12.81 dB, b) result of proposed method with Daubechies 8 at SNR = 18.8988 dB, c) result of VisuShrink at SNR = 16.2837 dB, d) result of BayesShrink at SNR = 18.4893 dB, e) result of SureShrink at SNR = 17.7961 dB, g) result of level-dependent threshold estimator with Daubechies 8 at SNR = 14.4218 dB.

Table 2. The performance (SNR) of the proposed method and others for the ECG signal (MIT-BIH database record 103) corrupted with Gaussian noise.

Input SNR	Output SNR proposed method			Output SNR for level-dependent threshold estimation			Output SNR for VisuShrink	Output SNR for SureShrink	Output SNR for BayesShrink
	DB4	DB6	DB8	DB4	DB6	DB8			
6.8	12.20	11.83	12.03	11.81	11.38	8.76	10.50	10.82	10.54
9.29	14.52	14.16	14.45	13.55	12.87	10.72	12.73	13.24	12.88
12.81	17.78	17.42	17.75	15.84	15.07	13.11	15.84	16.57	15.99
15.83	20.47	20.28	20.54	18.02	17.86	15.08	18.31	19.25	18.33

Table 3. The performance (SNR) of the proposed method and others for the ECG signal (MIT-BIH database record 103) corrupted with electrode motion noise.

Input SNR	Output SNR proposed method			Output SNR for level-dependent threshold estimation			Output SNR for VisuShrink	Output SNR for SureShrink	Output SNR for BayesShrink
	DB4	DB6	DB8	DB4	DB6	DB8			
6.8	10.97	10.88	11.17	10.21	10.28	10.14	9.45	10.85	10.72
9.29	13.36	13.23	13.54	12.36	12.26	12.28	11.65	13.27	13.05
12.81	16.64	16.64	16.78	15.20	14.91	15.02	15.74	16.60	16.14
15.83	19.49	19.51	19.57	17.29	16.71	16.95	17.34	19.31	18.48

Table 4 presents the SNR of the proposed method and the other methods for the ECG signals (MIT-BIH database record 103) corrupted with muscle artifact noise.

Table 4. The performance (SNR) of the proposed method and others for the ECG signal (MIT-BIH database record 103) corrupted with muscle artifact noise.

Input SNR	Output SNR proposed method			Output SNR for level-dependent threshold estimation			Output SNR for VisuShrink	Output SNR for SureShrink	Output SNR for BayesShrink
	DB4	DB6	DB8	DB4	DB6	DB8			
6.8	13.10	12.58	13.31	11.61	11.57	10.65	11.15	12.88	12.68
9.29	15.43	15.07	15.66	13.43	13.25	12.36	13.24	15.26	14.91
12.81	18.62	18.52	18.89	15.82	15.46	14.42	16.28	18.48	17.79
15.83	21.32	21.39	21.53	17.25	17.36	16.72	18.74	21.02	19.85

Table 5 lists the SNR of the proposed method and the others for the ECG signals (MIT-BIH database record 109) corrupted with electrode motion noise.

Table 5. The performance (SNR) of the proposed method and others for the ECG signal (MIT-BIH database record 109) corrupted with electrode motion noise.

Input SNR	Output SNR proposed method			Output SNR for level-dependent threshold estimation			Output SNR for VisuShrink	Output SNR for SureShrink	Output SNR for BayesShrink
	DB4	DB6	DB8	DB4	DB6	DB8			
6.8	10.92	10.96	10.94	10.53	10.74	10.62	10.57	10.91	10.85
9.29	13.30	13.37	13.35	12.66	12.88	12.76	12.77	13.26	13.22
12.81	16.43	16.69	16.78	15.49	15.57	15.39	15.76	16.65	16.62
15.83	19.41	19.67	19.77	17.38	17.53	17.27	18.25	19.28	19.19

Table 6 lists the SNR of the proposed method and the others for the ECG signals (MIT-BIH database record 117) corrupted with muscle artifact noise.

Table 6. The performance (SNR) of the proposed methods and others for the ECG signal (MIT-BIH database record 117) corrupted with muscle artifact noise.

Input SNR	Output SNR proposed method			Output SNR for level-dependent threshold estimation			Output SNR for VisuShrink	Output SNR for SureShrink	Output SNR for BayesShrink
	DB4	DB6	DB8	DB4	DB6	DB8			
6.8	12.97	12.67	13.13	13.42	12.58	12.68	12.99	12.99	12.98
9.29	15.50	15.31	15.59	15.61	14.32	14.76	15.25	15.50	15.48
12.81	19.08	19.00	19.37	18.65	16.25	17.60	18.38	18.98	18.96
15.83	21.97	21.96	22.04	20.97	17.32	19.86	21.43	21.99	21.95

The results clearly indicate that the proposed method has stronger denoising abilities than the others methods. Although the other methods removed the noise, the signal was distorted, as well. The analysis of these tables reveals some difference between the wavelet filters. Our method showed good performance with a DB8 filter. The values obtained from our proposed method were always among the ones that had the highest SNR.

In addition, we compared the execution time of the proposed method with those of the others. The results are listed in Table 7. To measure execution time, we measured CPU time at the beginning of execution and at the end of execution. We then computed the difference between them as the execution time.

Table 7. The execution time of the proposed method and others.

Input SNR (dB)	Execution time in seconds					
	Proposed method			VisuShrink	SureShrink	BayesShrink
	DB4	DB6	DB8			
6.8	0.125	0.140	0.141	0.2030	0.1870	0.3290

As seen in Table 7, the lifting scheme provides fast implementation of the wavelet transform. It has the further advantage of reduced computational complexity, as compared with classical wavelet transform.

3. Discussion

We have proposed a new method for electrocardiogram (ECG) denoising on a bivariate shrinkage function exploiting the interscale dependency of wavelet coefficients. As indicated in Section 2.3, there were strong dependencies between the coefficients and their parents in detail, so we considered the dependencies between the coefficients and their parents in detail on a bivariate shrinkage function for denoising of an ECG signal corrupted by different types of noises, such as muscle artifact noise, electrode motion, and white noise. The experiments were conducted on different ECG records from the MIT-BIH arrhythmia database. It was clearly seen in all Figures that we had separated the ECG signals and the noises over all frequency bands. Therefore, the P-, R-, and T-waves were more consistently identified. The effects of increasing the number of decomposition levels and the different kinds of transform on the proposed algorithm were investigated. We concluded that for higher decomposition levels, no improvement in SNR was obtained. Computational complexity is an important issue in real-time applications, so we utilized lifting-based wavelet transform because it speeds up the implementation of the ECG denoising method. In addition, different lifting-based wavelet filters, such as DB4, DB6, and DB8, were used to assess the performance of the proposed method. We had the highest SNR values with the proposed method by DB8.

References

[1] J.D. Bronzino, The Biomedical Handbook, Vol. 1, 2nd ed., Boca Raton, FL, CRC, 2000.

[2] S.A.P. Haddad, R.P.M. Houben, W.A. Serdijin, "The evolution of pacemakers", IEEE Engineering in Medicine and Biology Magazine, Vol. 25, pp. 38-48, 2006.

[3] J.W. Tukey, "Nonlinear methods for smoothing data", Congr. Rec. 1974 EASCON, p. 643, 1974.

[4] J. Pitas, A.N. Venetsanopoulos, "Order statistics in digital image processing", Proc. IEEE Vol. 80, pp. 1893-1921, 1992.

[5] J.E.A. Sheild, D.L. Kirk, "The use of digital filters in enhancing the fetal electrocardiogram", J. Biomed. Eng., Vol. 44, pp. 44-48, 1981.

[6] E.H. Hon, S.T. Lee, "Noise reduction in fetal electrocardography, II. Averaging techniques", Am. J. Obstet. Gynecol., Vol. 87, pp. 1086-1096, 1963.

[7] S. Mallat, S. Zhong, "Characterization of signal from multiscale edges", IEEE Trans. on Pattern Analysis and Machine Intelligence, Vol. 14, pp. 701-732, 1991.

[8] N.J. Qutram, E.C. Ifeachor et al., "Techniques for optimal enhancement and feature extraction of fetal electrocardiogram", IEE Proc.-Sci. Meas. Technol., Vol. 142, pp. 482-489, 1995.

[9] W. Gao, H. Li, Z. Zhuang, T. Wang, "Denoising of ECG signal based on stationary wavelet transform," Acta Electronica Sinica, Vol. 32, pp. 238-240, 2003.

[10] L. Su, G. Zhao, "Denoising of ECG signal using translation-invariant wavelet denoising method with improved thresholding", Proceedings of the 2005 IEEE Engineering in Medicine and Biology 27th Annual Conference, Shanghai, pp. 5946-5949, 2005.

[11] D.L. Donoho, I.M. Johnstone, "Ideal spatial adaptation via wavelet shrinkage", Biometrika, Vol. 81, pp. 425-455, 1994.

[12] D.L. Donoho, "Denoising by soft-thresholding", IEEE Trans. Inform. Theory, Vol. 41, pp. 613-627, 1995.

[13] R.R. Coifman, D.L. Donoho, "Translation-invariant denoising", in: Wavelets and Statistics, Springer Lecture Notes in Statistics 103, New York, Springer-Verlag, pp. 125-150, 1994.

[14] E. Erçelebi, "Electrocardiogram signals denoising using lifting-based discrete wavelet transform", Computers in Biology and Medicine, Vol. 34, pp. 479-493, 2004.

[15] D.L. Donoho, I.M. Johnstone, "Adapting to unknown smoothness via wavelet shrinkage", J. Amer. Statist. Assoc., Vol. 90, pp. 1200-1224, 1995.

[16] S. Chang, B. Yu, M. Vetterli, "Adaptive wavelet thresholding for image denoising and compression", IEEE Trans. Image Processing, Vol. 9, pp. 1532-1546, 2000.

[17] C.M. Stein, "Estimation of the mean of a multivariate normal distribution", Ann. Statist., Vol. 9, pp. 1135-1151, 1981.

[18] B.N. Singh, A.K. Tiwari, "Optimal selection of wavelet basis function applied to ECG signal denoising", Digital Signal Processing, Vol. 16, pp. 275-287, 2006.

[19] L. Şendur, I.W. Selesnick, "Bivariate shrinkage functions for wavelet-based denoising exploiting interscale dependency", IEEE Trans. on Signal Proc., Vol. 50, pp. 2744-2756, 2002.

[20] M.A.T. Figueiredo, R.D. Nowak, "Wavelet-based image estimation: An empirical Bayes approach using Jeffrey's noninformative prior", IEEE Trans. Image Processing, Vol. 10, pp. 1322-1331, 2001.

[21] H. Gao, "Wavelet shrinkage denoising using the nonnegative garrote", J. Comput. Graph. Stat., Vol. 7, pp. 469-488, 1998.

[22] A. Hyvarinen, "Sparse code shrinkage: Denoising of nongaussian data by maximum likelihood estimation", Neural Comput., Vol. 11, pp. 1739-1768, 1999.

[23] A. Hyvarinen, E. Oja, P. Hoyer, "Image denoising by sparse code shrinkage", in: Intelligent Signal Processing, S. Haykin and B. Kosko, Eds., Piscataway, NJ, IEEE, 2001.

[24] E.P. Simoncelli, E.H. Adelson, "Noise removal via Bayesian wavelet coring", Proc. IEEE Int. Conf. Image Process., Vol. 1, pp. 379-382, 1996.

[25] B. Vidakovic, Statistical Modeling by Wavelets, New York, Wiley, 1999.

[26] E.P. Simoncelli, "Bayesian denoising of visual images in the wavelet domain", in: Bayesian Inference in Wavelet Based Models, P. Müller and B. Vidakovic, Eds., New York, Springer-Verlag, 1999.

[27] MIT-BIH Arrhythmia Database CD-ROM, Cambridge, MA, Harvard-MIT Division of Health Sciences and Technology, 1997.

[28] A. Alesanco, S. Olmos, R. Istepanian, J. Garcia, "A novel real-time multilead ECG compression and denoising method based on the wavelet transform", Computers in Cardiology,;ol. 30, pp. 593-596, 2003.

[29] M. Vetterli, J. Kovaevi, Wavelets and Subband Coding, Englewood Cliffs, New Jersey, Prentice Hall PTR, 1995.

[30] K. Niijima, K. Kuzume, "Wavelets with convolution-type orthogonality conditions", IEEE Tran. Signal Processing, Vol. 47, pp. 408-421, 1999.

[31] I. Daubechies, W. Sweldens, "Factoring wavelet transforms into lifting steps", J. Fourier Anal. Appl., Vol. 4, pp. 245-267, 1998.

[32] W. Sweldens, "The lifting scheme: A new philosophy in biorthogonal wavelet constructions", Proceedings of SPIE, Vol. 2569, pp. 68-79, 1995.

[33] W. Sweldens, "The lifting scheme: A custom design of biorthogonal wavelets", Applied Computational and Harmonic Analysis, Vol. 3, pp. 186-200, 1996.

[34] E. Erçelebi, "Second generation wavelet transform-based pitch period estimation and voiced/unvoiced decision for speech signals," Applied Acoustics, Vol. 64, pp. 25-41, 2003.

[35] H. Liao, M.K. Mandal, B.F. Cockburn, "Novel architectures for the lifting-based wavelet transform", Proceedings of the 2002 IEEE Canadian Conference on Electrical & Computer Engineering, pp. 1020-1025, 2002.

[36] R. Senthilkumar, "Performance improvement in the bivariate models by using modified marginal variance of noisy observations for image-denoising applications", Trans. on Eng., Computing And Technology, Vol. 5, pp. 294-298, 2005.